A -195 dBc/Hz FoM$_T$ 20.8-to-28-GHz LC VCO with Transformer-Enhanced 30% Tuning Range in 65-nm CMOS

S. Lightbody*, A. H. M. Shirazi*, H. Djahanshahi#, R. Zavari#, S. Mirabbasi*, S. Shekhar*
*University of British Columbia, Canada
#Microsemi Corp., Canada

***Abstract*— Low quality factor (Q) of varactors and increased ratio of parasitic capacitance to total tank capacitance impede the design of high-frequency voltage-controlled oscillators (VCOs) that must attain wide frequency tuning range (FTR) and low phase noise (PN). We propose a VCO topology which instead of directly connecting a varactor to the oscillator core, leverages a transformer to magnetically couple the varactor to the core. This approach increases the tuning range of the varactor by doubling the bias range, further reduces the parasitic capacitance seen by the varactor, and boosts the resonator tank Q due to impedance transformation. Thus, both PN and FTR are improved simultaneously. Measurement results for the prototype VCO implemented in 65-nm CMOS show an FTR of 29.8% from 20.77 to 28.02 GHz while consuming 12.65 to 15.12 mW. A PN of -106.6 dBc/Hz at a 1 MHz offset and an FoM$_T$ of -195 dBc/Hz are attained.**

***Index Terms*— Class-C, low phase noise, transformer, wide tuning range.**

I. INTRODUCTION

Emerging wireline and optical standards demand data rates up to 56 Gbaud/s, often with support for lower speeds such as 28/10/5 Gbaud/s. Supporting this wide range of data rates has required a combination of multiple VCOs and frequency dividers and multipliers [1]. Multiple VCOs are used because low phase noise (PN) and wide frequency tuning range (FTR) are difficult to be simultaneously achieved in CMOS VCOs operating at high frequencies [2]. However, multiple LC VCOs lead to increase in the number of inductors, frequency synthesizers, silicon area and design complexity [2]. A single, wide FTR LC-VCO that operates with low PN from 20-to-28 GHz to support such data rates with only frequency dividers is the focus of this work.

Achieving these requirements while operating in the 10s of GHz range has been a significant challenge due to (i) the degraded performance of the varactor, which has a quality factor (Q) inversely proportional to the frequency of operation (f_0) [3], (ii) degraded performance of switchable capacitor banks, and (iii) higher ratio of parasitic capacitance to variable capacitance in the tank. There have been many attempts to address these issues [3], [4], [5], [6], however, the FTR with low PN remains moderate at best.

Transformer-based resonators have been studied thoroughly in recent years [7], [8]. In [7], the primary and secondary of the transformer are designed as loads which are nearly identical in terms of their respective Q (Q$_p$ and Q$_s$) and resonant frequency while switched current sources allow either the higher or lower frequency mode of the transformer to be excited, boosting the effective FTR. However, this design suffers from the decreased performance in the higher frequency mode and is not able to take advantage of the magnetic decoupling of passive components. In this work, we investigate the several benefits of coupling imbalanced loads by moving all low-Q varactors to the secondary node of the transformer, away from the primary switching core and power supply, in an effort to maximize FTR and the tank Q (Q$_T$) and improve PN. Although only the lower frequency mode of the resonator is used a significantly large and gapless FTR is achieved.

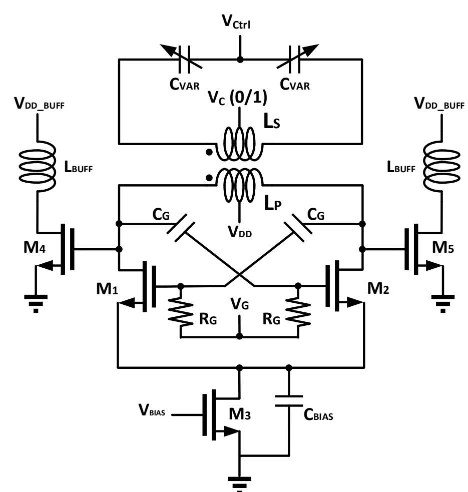

Fig. 1. A Class-C VCO with transformer enhanced tuning range and tank Q

II. DESIGN CONSIDERATIONS

A. Schematic Overview

The proposed design schematic is shown in Fig. 1. A Class-C VCO is implemented with a resonator made up of a transformer coupling two LC-tanks with a coupling constant k. Frequency control is achieved by setting the voltage across the varactors C$_{VAR}$ with the pins V$_{Ctrl}$ and V$_C$. V$_{Ctrl}$ is varied from 0 to V$_{DD}$ while V$_C$ can be switched in a discrete fashion between 0 and V$_{DD}$ to extend the capacitance variation. Such a switching is easily realizable in synthesizers, in a fashion similar to switchable capacitor banks, but without the performance degradation of the latter.

B. Q-Enhancement from Transformer

Fig. 2(a) shows a conventional LC resonator tank with tank inductor, varactor C_{VAR}, and parasitic capacitance C_{PAR}. Fig. 2(b) shows the transformer-enhanced resonator tank used in the VCO. The resonant frequency ω_p of the primary side of the tank is defined by the inductance of the primary winding L_P and the parasitic capacitance associated with the VCO switching core and buffers, while the resonant frequency ω_s of the secondary is defined solely by the inductance L_S of the secondary along with C_{VAR}. We know from [7] that the magnetic fields produced by either side of the transformer can couple in phase proportional to k, increasing the stored energy in the resonator. This causes the VCO to oscillate at ω_0 given by

$$\omega_0 = \Omega(\xi, k)\omega_s \tag{1}$$

where

$$\Omega(\xi, k) = \sqrt{\frac{1 + \xi - \sqrt{(1-\xi)^2 - 4\xi(1-k^2)}}{2(1-k^2)}} \tag{2}$$

and

$$\xi = (\frac{\omega_p}{\omega_s})^2. \tag{3}$$

For this design, it is important to note that because of the effect of increased inductance seen at the primary in the lower frequency mode, ω_0 will always be lower than both ω_p and ω_s regardless of the value of ξ or k [7].

The extra magnetic energy storage can act to increase the quality factor at ω_0 of the transformer tank, Q$_T$, beyond the value of Q$_p$ and Q$_s$ [7], [8]. The improvement in quality factor $\frac{Q_T}{Q_p}$ is proportional to k and is a function of $\frac{Q_p}{Q_s}$ as well as ξ.

In this design, the placement of the varactor on the secondary results in $Q_s < Q_p$. For this case of $\frac{Q_p}{Q_s} > 1$, the optimum ξ shifts below unity leading to Q_T to be boosted near or above Q_p (which is itself improved due to the omission of the varactor) for high values of ω_s [8]. Fig. 3(a) shows the boost factor $\frac{Q_T}{Q_p}$ due to the transformer action for $\frac{Q_p}{Q_s} = 1.4$. As ω_s is tuned, ξ varies with it (from (3)), so this boosting is limited to a certain frequency range. However, for a proper choice of ξ, it is held above 1 for the required FTR of ω_s.

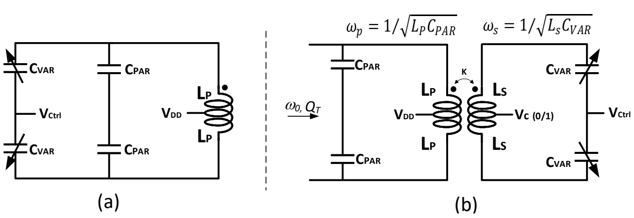

Fig. 2. (a) Conventional LC resonator, and (b) Transformer-enhanced resonator

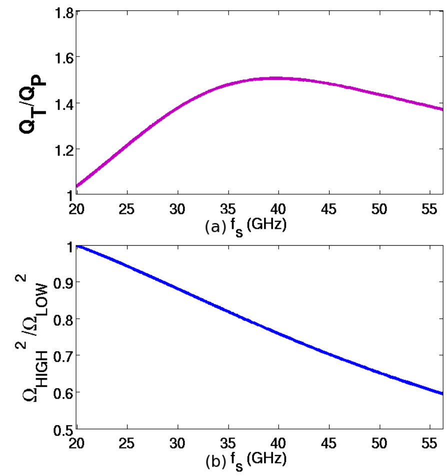

Fig. 3. Plot of (a) $\frac{Q_T}{Q_p}$ for $\frac{Q_p}{Q_s}$ = 1.4 and (b) $\frac{\Omega_{HIGH}}{\Omega_{LOW}}$ vs. f_s

The enhancement in Q_s due to the transformer action comes with a trade-off in FTR reduction. As the effect of the varactor loss on the whole tank is reduced, the effect of its capacitance variation on FTR is reduced as well. From (1) we can see that ω_0 is ω_s scaled by some coefficient Ω, which is a function of ξ. Since ξ will vary as ω_s varies, Ω will scale ω_s differently at different frequencies. If Ω decreases as ω_s increases, a compression effect on the FTR of ω_0 from ω_s is observed. It can be shown that

$$TR_{\omega_0} = \frac{\Omega_{HIGH}}{\Omega_{LOW}} * TR_{\omega_s} \tag{4}$$

where $\frac{\Omega_{HIGH}}{\Omega_{LOW}}$ is the ratio of Ω at the highest and lowest frequencies of the tuning range, and TR is the ratio of the highest and lowest frequency in the range.

Fig. 3(b) shows that Ω decreases with decreasing ξ (or increasing ω_s), with the decrease becoming more pronounced the further ω_s is tuned. Based on this load analysis, the FTR is diminished. However, there are benefits to decoupling the varactor from the supply and core transistors using the transformer which are not captured by a load analysis. Next, we show that FTR can be also simultaneously enhanced in our design.

C. Varactor Performance Enhancement

In a standard VCO design, a varactor is usually connected to a control voltage V_{Ctrl} on one end and some V_{DD}-dependent voltage on the other end depending on the implementation of the switching transistors (see

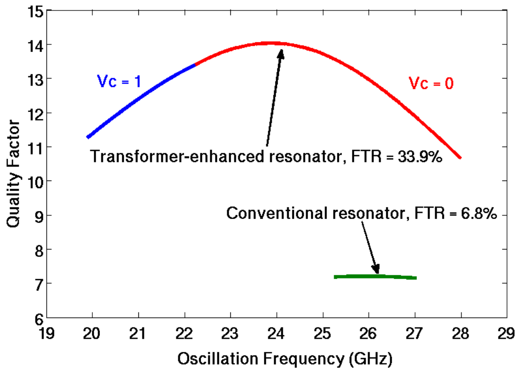

Fig. 4. Plot of Q_T vs. oscillation frequency for a transformer-enhanced resonator and a conventional resonator

Fig. 2(a)). V_{Ctrl} can be varied arbitrarily, but the other node must be held constant to allow operation of active components in the circuit. Capacitance variation can be increased by increasing the range of V_{Ctrl} above V_{DD} or below GND, but large bias voltages and negative voltages may be challenging to be produced on-chip. By magnetically coupling the varactor to the tank, we remove this power supply constraint from the passives and free the second pin of the varactor to be biased through the centre pin of the secondary winding with voltage V_C. If V_{Ctrl} is a voltage bounded between V_{DD} and GND then the voltage tuning range measured across the varactor can be almost doubled by switching V_C between V_{DD} and GND in a binary fashion. This has the effect of adding a second frequency band to tune V_{Ctrl} across.

Separating the varactor from the active circuitry also improves the varactor performance by significantly reducing the amount of parasitic capacitance seen at the resonant node. Any fixed parasitic capacitance attenuates the effect of C_{VAR} on the overall FTR. By disconnecting the varactor from the transistors we are able to attenuate the parasitic capacitance seen by the varactor in the secondary. This allows the TR of ω_s to reach extremely high percentages for the same varactor sizing, or the same TR for a much higher Q. However, as previously mentioned, there is a partial reduction in the tank FTR caused by the transformer coupling.

Fig. 4 shows a simulated comparison between FTR and quality factor of a transformer-enhanced resonator and a conventional LC resonator that use the same varactor varying V_{Ctrl} from 0 to 1 V. In the conventional LC resonator, the secondary winding is removed and the varactor is connected in parallel with the primary inductor while all other components are kept constant. The transformer resonator is simulated with a small parasitic capacitance of 10 fF on the secondary, consistent with post-layout simulations. The blue and red portion of the transformer tuning curve correspond to V_C set to 1 V and 0 V, respectively. We observe that both quality factor of the transformer resonator and FTR are larger than a conventional LC resonator with the same varactor.

III. Design and Measurement Results

A prototype of the proposed VCO is designed in 65-nm CMOS. The die micrograph is shown in Fig. 5. The transformer is designed to maximize k, which is 0.76 across the range. L_P is a single large winding to increase Q. L_S is implemented with two windings in order to decrease the varactor size while still keeping ω_s to reasonable values. Since $\omega_0 < \{\omega_p, \omega_s\}$, ω_p is designed to be slightly above the maximum desired frequency. In order to minimize the reduction in FTR due to (4), ω_s is designed to tune around ω_p, keeping ξ close to unity. ω_s is designed to never tune to such a low frequency so that $\xi > 3$, as this would risk a higher-order oscillation [7].

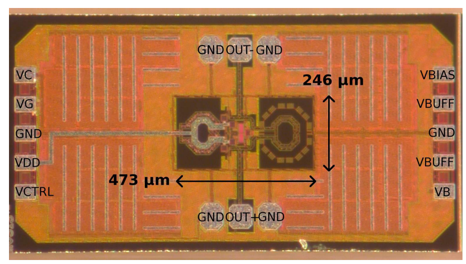

Fig. 5. Chip micrograph of VCO showing core area of 246 x 473 μm^2

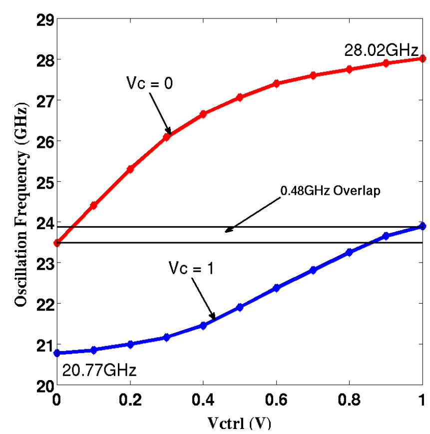

Fig. 6. Measured VCO oscillation frequency vs control voltage

The prototype is measured using an R&S FSWP-50 spectrum and PN analyzer. Fig. 6 shows the FTR plot of the VCO, achieving a frequency range of 20.77 GHz to 28.02 GHz (FTR of 29.8%) while consuming a core power P_{DC} of 12.65 mW to 15.12 mW from a 1 V supply. Fig. 7 shows the PN plot at 26.45 GHz with a PN of -106.6 dBc/Hz at $\Delta f = 1$ MHz offset. An overlap of 480 MHz is achieved between the two frequency bands by altering the bias. If more overlap is

TABLE I
PERFORMANCE SUMMARY AND COMPARISON

Parameters	**This Work**	**[4]**	**[5]**	**[3]**	**[6]**
Architecture	XFMR Enhanced	Switchable Coupled Cores	Standing Wave	Self-Mixing	XFMR Coupled QVCO
Frequency (GHz)	20.77 to 28.02	55.7 to 66	26.3 to 27.6	52.8 to 62.5	14.8 to 17.6
FTR %	29.8	17.2	4.8	16.8	16.5
V_{Ctrl} Range (V)	0 to 1	0 to 2.4	0 to 3.3	0 to 1.8	0 to 1.8
V_{DD}(V)	1	1.2	1.8	1.2	1
PN (dBc/Hz) @1MHz	-106.6	-93.5	-115	-100.57	-110
P_{DC}(mW)	12.65 to 15.12	19.1/11.2	17.7	7.6	5
Technology Node	65-nm CMOS	180-nm BiCMOS	180-nm CMOS	130-nm CMOS	180-nm CMOS
F_OM (dBc/Hz) @ 1MHz	-185.5	-176.3	-191	-186.3	-187.6
F_OM_T (dBc/Hz) @ 1MHz	-195	-181	-184.62	-190.85	-191.94

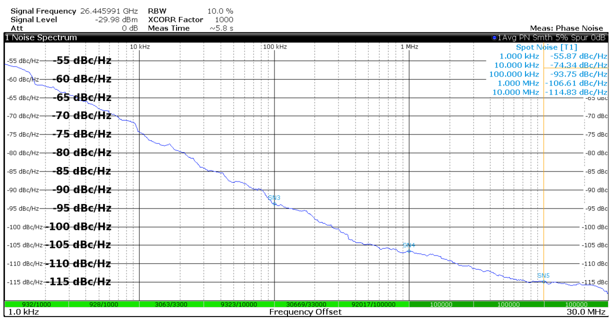

Fig. 7. Measured phase noise at 26.45 GHz

desired, V_C can be generated using a voltage DAC to implement several intermediate frequency bands, similar to those obtained using a capacitor DAC but without the performance degradation of the latter. The variation in K_{VCO} across the TR can be compensated by charge pump current linearization techniques in the PLL [9].

Table I provides a performance comparison of the transformer-enhanced varactor VCO to other state-of-the-art high-frequency VCO designs. Designs are compared using the popular Figure-of-Merit (FoM) equation as well as the FTR-inclusive FoM_T [3]:

$$FoM = PN - 20log(\frac{f_0}{\Delta f}) + 10log(\frac{P_{DC}}{1mW}) \quad (5)$$

$$FoM_T = FoM - 20log(\frac{FTR}{10\%}) \quad (6)$$

IV. CONCLUSION

Connecting a varactor to the secondary of a transformer can increase the tank Q, significantly reduce the parasitics in the secondary tank and thereby enable the varactor to control most of the frequency tuning, and enable flexible biasing for the varactor. Thus, PN and FTR can be simultaneously improved, significantly relaxing the tradeoff associated with high-frequency VCO designs. A 20.77-to-28.02 GHz prototype demonstrates the benefits of the proposed techniques and achieves the lowest FoM_T of -195 dBc/Hz reported for VCOs in high-frequency range. The techniques are suitable for multi-rate wireline/optical transceivers, as well as attractive for high-frequency 5G radio bands.

ACKNOWLEDGEMENTS

The authors acknowledge NSERC, Intel and Microsemi for financial support, CMC for access to CAD tools, Rohde & Schwarz for test equipment, and R. Mehrabadi and Dr. R. Rosales for CAD and test support.

REFERENCES

[1] T. Musah *et al.*, “A 4-32 Gb/s bidirectional link with 3-tap FFE/6-tap DFE and collaborative CDR in 22 nm CMOS,” *IEEE J. Solid-State Circuits*, pp. 3079–3090, Dec. 2014.

[2] F. Shirinfar *et al.*, “A multichannel, multicore mm-wave clustered VCO with phase noise, tuning range, and lifetime reliability enhancements,” in *IEEE Radio Freq. Intgr. Circuits Symp.*, June 2013, pp. 235–238.

[3] A. Shirazi *et al.*, “On the design of mm-wave self-mixing-VCO architecture for high tuning-range and low phase noise,” *IEEE J. Solid-State Circuits*, pp. 1210–1222, May 2016.

[4] Q. Zou *et al.*, “A low phase noise and wide tuning range millimeter-wave VCO using switchable coupled VCO-cores,” *IEEE Trans. Circuits Sys. I*, pp. 554–563, Feb. 2015.

[5] T.-H. Huang and P.-L. You, “27-GHz low phase-noise CMOS standing-wave oscillator for millimeter wave applications,” in *IEEE Int. Microwave Symp.*, June 2008, pp. 367–370.

[6] A. W. L. Ng and H. C. Luong, “A 1-V 17-GHz 5-mW CMOS quadrature VCO based on transformer coupling,” *IEEE J. Solid-State Circuits*, pp. 1933–1941, Sep. 2007.

[7] A. Bevilacqua *et al.*, “Transformer-based dual-mode voltage-controlled oscillators,” *IEEE Trans. Circuits Sys. II*, pp. 293–297, Apr. 2007.

[8] A. Mazzanti and A. Bevilacqua, “On the phase noise performance of transformer-based CMOS differential-pair harmonic oscillators,” *IEEE Trans. Circuits Sys. I*, pp. 2334–2341, Sep. 2015.

[9] T. Wu *et al.*, “Method for a constant loop bandwidth in LC-VCO PLL frequency synthesizers,” *IEEE J. of Solid-State Circuits*, vol. 44, no. 2, pp. 427–435, Feb 2009.